Cellulose (2012) 19:81–90
DOI 10.1007/s10570-011-9627-7

Nematic ordered cellulose templates mediating order-patterned deposition accompanied with synthesis of calcium phosphates

Koki Higashi · Tetsuo Kondo

Received: 29 June 2011 / Accepted: 23 November 2011 / Published online: 3 December 2011

Abstract In a previous study, the nematic ordered cellulose (NOC) templates successfully induced biodirected epitaxial nanodeposition of cellulose nanofibers secreted by *Gluconacetobacter xylinus* along the orientation of the molecular tracks (Kondo et al. 2002). As an extended concept for the NOC, this article attempts to propose a sort of biomimic mineralization using the template. It combines morphologically controlling process with synthesis of the calcium phosphate as a major component of bones. This process was initially mediated by the modified NOC template having a pair of roles of the ion supply sources and scaffolds for 3D-ordering architecture of the calcium phosphate as a biomineral in the key functions for biomineralization. The successful establishment of such an ordered deposition of the inorganic on the template was confirmed by several surface characterizations such as atomic force microscopy, X-ray photoelectron spectroscopy, scanning electron microscopy, and so on. Moreover, similarly to human bones, the obtained major assemble states of the calcium phosphates exhibited amorphous. The above process using the bifunctional cellulose template can be considered as a biomimic mineralization, which also opens pathways toward preparation of potentially versatile organic–inorganic order-patterned composites under a less energy consumption.

Keywords Nematic ordered cellulose · Order-patterned deposition · Calcium phosphate · Biomimic mineralization · Orientation

K. Higashi · T. Kondo (✉)
Graduate School of Bioresource and Bioenvironmental Sciences, Kyushu University, 6-10-1, Hakozaki, Higashi-ku, Fukuoka 812-8581, Japan
e-mail: tekondo@agr.kyushu-u.ac.jp

Introduction

In biological systems, micro organisms such as cells and bacteria synthesize minerals for skeletal materials to support their bodies as bones and shells. The three-dimensional structures of mineral building blocks are hierarchically assembled upon organic scaffolds to express various functions for their survival. Such formation processes of organic–inorganic composites are called as biomineralization, while the inorganic salts are called biominerals (e.g. calcium phosphate, calcium carbonate, and silicon dioxide and so on) in the processes. The biomineral as a component is synthesized by an aqueous reaction between ions at ambient temperatures and pressures, and therefore the biomineralization can be considered as a less energy consumption system. The type, size, and shape of biominerals are mainly controlled by two factors, which are an ion supply source as well as the surface properties of an organic scaffold. The ion supply sources are in general sea water or blood plasma,

whereas the organic scaffolds comprise polysaccharides or proteins (Dorozhkin and Epple 2002).

In the case of human bones, the dominant component as a biomineral is hydroxyapatite (HAp: $Ca_{10}(PO_4)_6(OH)_2$) that is deposited along the surface of collagen fibrils. The morphology of HAp is also decided by the above two factors which are matrix vesicles as the ion supply source and ordered collagen fibrils as the scaffold, respectively. In this biomineralization process, the HAp formation starts with secretion of matrix vesicles from osteoblast cells. The individual vesicle is an organism that acts as the supply sources of essential phosphate anions for HAp fabrication. Following the vesicles deposited to collagen fibrils, the phosphate anions in the membrane of the vesicle are supposed to react with surrounding calcium cations in the plasma to form crystalline cores in and out of the membrane. The crystalline cores are normally amorphous calcium phosphates or poorly crystalline apatites, which are accelerated to be formed by the highly concentrated phosphate anions in the vesicles (Boskey and Posner 1977; Boyan et al. 1989; Anderson 1995; LeGeros 2002). Then the cores undergo several crystalline phase transitions to HAp. At the subsequent stage, the amorphous cores for crystallization gradually grow up and finally come out through the membrane of the vesicle to be deposited into collagen fibrils. As the deposition grows on ordered collagen fibrils as a scaffold, the size and shape of crystalline HAp begins to be perfectly arranged depending on the scaffold order (Rho et al. 1998), resulting in the toughness, despite the brittleness of HAp alone in vitro (Kim et al. 1996; Weiner and Wagner 1998; Dorozhkin and Epple 2002; Olszta et al. 2007). Here, it is noted that the HAp thus formed contains still highly amorphous phases (Roberts et al. 1991; Roberts et al. 1992). Studies on formation processes of organic–inorganic composites have been extensively conducted according to the concept of biomimicry; for example, mimicking the structure of scaffolds (Jie et al. 2005), the composition of ions (Kokubo 1990; Kokubo 2005) and the procedure of mineralization (Taguchi et al. 1998; Furuzono et al. 2000). None of such studies, however, have been focused on a pair of the functions of both ordered scaffolds and ion suppliers simultaneously.

In our previous paper, we reported a unique form of β-glucan association, nematic ordered cellulose (NOC) that is molecularly ordered, yet non-crystalline (Togawa and Kondo 1999; Kondo et al. 2001; Kondo 2007). Since the NOC is prepared by uniaxial stretching of water-swollen cellulose, the amphiphilic cellulose molecular chains tend to be oriented toward the stretching axis, resulting in forming uniaxially amphiphilic molecular tracks on the surface. The unique surface structure induces orientation of deposition of cellulose nanofibers secreted by *Gluconacetobacter xylinus*, a gram-negative bacterium (Kondo et al. 2002; Kondo 2007).

In this study, the authors attempt to propose a novel type of biomineralization process by developing a bifunctional cellulose template. Namely, the NOC template has been modified into a bifunctional template having a pair of the functions required for biomineralization, resulting in inducing oriented deposition of the calcium phosphates as well as supplying phosphate ions in the synthesis. The new NOC template that is prepared to contain phosphate anions (p-NOC) is expected to mediate a unique order patterned deposition of calcium phosphates on the surface by reaction with calcium cations during immersion in a buffer solution. Such arranged morphology of the calcium phosphates, if possible, would be formed at room temperature, leading to a biomimic mineralization in terms of a lower energy consumption process.

Experimental

Materials

Bleached cotton linters with a degree of polymerization (DP) of 1,300 were used as the starting cellulose sample. N, N-Dimethylacetamide (DMAc) and lithium chloride (LiCl) were purchased from Wako Pure Chemical Industries, Ltd. to prepare the solution for dissolution of the cellulose.

Preparation of nematic ordered cellulose templates containing phosphate anions (p-NOC)

Dissolution of the cellulose and preparation of a water-swollen cellulose gel was followed by a previous procedure using DMAc/LiCl solvent system (Togawa and Kondo 1999; Kondo et al. 2001). The water-swollen cellulose gel was immersed in phosphate buffered saline (PBS, Sigma-Aldrich co., Ltd.) for 1 week to prepare a water-swollen cellulose gel containing phosphate anions.

The gel-like films containing phosphate anions above prepared were cut into strips approximately 30 mm long and 10 mm wide, and then the strips were elongated uniaxially to a draw ratio of 2.0 at room temperature. In the drawing process, the specimen was kept in a wet state by pouring the PBS on the surface of the film. After the drawing was completed, the specimen was air-dried for 24 h and then vacuum-dried at 25 °C for more than 48 h. As a reference, non-ordered cellulose templates containing phosphate anions (p-cellulose) was prepared by the same procedure for p-NOC, except the stretching process. The two types of the films containing phosphate anions above prepared were clamped the four corners with fixing device to prevent them from shrinking on the drying process described above.

Synthesis and deposition of calcium phosphates on cellulose templates

Two types of films thus prepared were immersed to encourage the reaction of phosphate anions with calcium cations on the surfaces in 20 mM of $CaCl_2$/Tris–HCl (calcium buffer solution) with pH 7.5 at 37 °C for 10 min. Following the specimen was rinsed by a sufficient amount of extra-pure water to remove excess calcium cations from the surface of the film, the specimen was air-dried for 24 h and then vacuum-dried at 25 °C for more than 48 h.

Characterization methods

Atomic force microscopy (AFM)

AFM images of the template surfaces were acquired on SPM-9500J3 (Shimazu Co. Ltd.). AFM was performed at room temperature, being controlled in the contact mode with a scan rate from 1 to 1.5 Hz to observe 5 × 5 μm^2 areas. An etched-silicon tip with a nominal radius less or equal 20 nm having a cone angle of 35° was employed for the AFM tip. In this observation, as height of the aggregates was smaller than radius of the tip, the following correction equation was employed:

$$E = 2 \times (RH - H^2)^{1/2},\ w = W - E,$$

where E is the geometrical enhancement on the real width value (w), W is the apparent width observed in AFM, H is the height of the object observed in AFM, and R is value of 20 nm in the AFM tip radius (Kondo 2007).

X-ray photoelectron spectroscopy (XPS)

XPS analysis was performed with AXIS-HSi spectrometer (Shimazu/Kratos Co. Ltd.). XPS spectra were obtained using a monochromatic Al Kα X-ray source (1,486.6 eV) at a voltage of 15 kV and a current of 10 mA. The vacuum level of the analyzing chamber was maintained below 7.0×10^{-7} Pa during the measurements. The pass energy and step width during the survey scan were set at 80 and 1.0 eV, respectively (Yokota et al. 2007).

Scanning electron microscopy (SEM)-Energy dispersive X-ray analysis (EDX)

All SEM-EDX micrographs of the surface of cellulose templates were obtained with a JSM5600LV scanning electron microscope (JEOL Ltd.) equipped with a JED-2140 energy dispersive X-ray microanalyzer (JEOL Ltd.). Samples were coated with carbon on a JEC-520 carbon coater (JEOL Ltd.) to achieve optimal imaging results. SEM images were acquired at 5–10 kV of the accelerating voltage, whereas EDX analyses were performed at 15 kV with the take-off angle under 30° unless otherwise specified.

Wide angle X-ray diffraction (WAXD)

The crystalline structures of calcium phosphates were determined by WAXD analysis using an XD-D1 X-ray diffractometer (Shimazu Co. Ltd.). WAXD patterns were acquired using Ni-filtered Cu Kα radiation (λ=1.5418Å) at a voltage of 30 kV and a current of 40 mA, in the scanning range from 20 to 40° at a diffraction range of 2θ.

Results and discussion

Surface morphology of reacted cellulose templates

Prior to the reaction and deposition of inorganics by immersion, the initial surface morphology of two types of cellulose templates containing phosphate anions together with the original NOC substrate were

investigated by using AFM. In comparison between Fig. 1a and b, the AFM images of height mode demonstrated that p-NOC containing phosphate anions possessed well-ordered surface morphology along the stretching direction similar to the original NOC substrate. Further, the polarized distribution of spots in the two-dimensional fast Fourier transformed (2D-FFT) image inserted in Fig. 1b confirmed a high degree of uniaxial orientation on the surface of p-NOC. The average line width was calculated from the cross-section analyses of the height along the A–B line perpendicular to the stretching direction (see the bottom figures in Fig. 1). The average distance between two parallel cellulose chains was 0.14 ± 0.03 μm ($n = 50$) in the p-NOC template surface (Fig. 1b). The line width was similar to that of the original NOC template 0.17 ± 0.06 μm ($n = 50$) as shown in Fig. 1a, indicating that a physical association of cellulose chains was not interfered even if phosphate anions existed in the p-NOC template. In addition, the negatively polarized surface due to the tracks of OH groups along the molecular orientation is supposed to appear to some extent on the surface of the original NOC (Kondo et al. 2001, 2002; Kondo 2007). Thus, if phosphate anions are contained in NOC templates, then they are likely to be immobilized on the glucose planes between the OH tracks in the surface. Accordingly, the phosphate anions are also supposed to be aligned along the molecular tracks in the newly prepared p-NOC template.

Without stretching of the gel containing phosphate anions, a non-ordered structure was observed on the surface of the p-cellulose whose 2D-FFT image confirmed its non-oriented surface morphology as shown in Fig. 1c. By uniaxial stretching of the cellulose gel, it was considered that the stretched template (termed as p-NOC) resulted in having the unique surface morphology similar to NOC that is totally different from the non-ordered p-cellulose template. Surface analyses for each template were performed to demonstrate the difference of the resultant surface morphology depending on the template. The root-mean-square (RMS) volumes were calculated from the obtained AFM height images to compare the surface roughness of each template. The RMS values for p-NOC and p-cellulose corresponded to 8.3 nm and 6.2 nm, respectively. Namely, p-NOC exhibited a significantly rougher surface than p-cellulose. The results from cross-section images with 2D-FFT together with the RMS analyses demonstrated that the p-NOC had the orientated, but relatively rough surface in comparison with the p-cellulose. In our previous paper, the NOC was found to induce the orientation of cellulose nanofibers secreted by *G. xylinus* on its surface (Kondo et al. 2002; Kondo 2007). It seemed therefore that an anionic p-NOC surface also might induce the orientation of other substances containing cationic ions. Thus, the effect of surface morphology of the modified NOC for a template-mediated mineralization was investigated

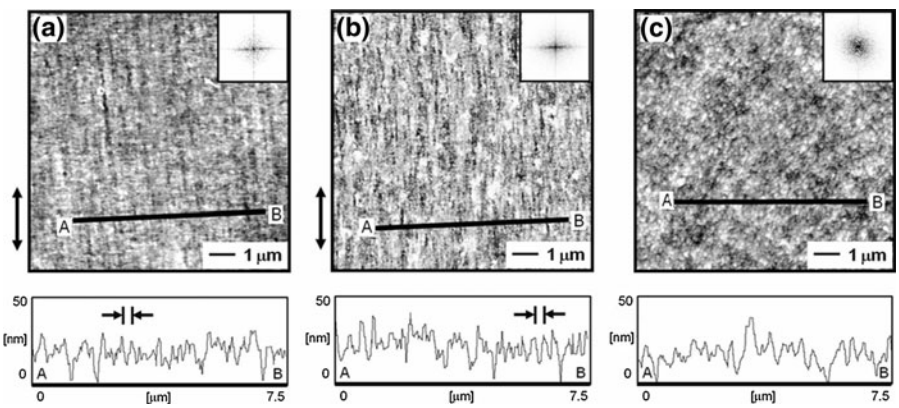

Fig. 1 AFM images of **a** NOC template, **b** p-NOC template and **c** non-ordered cellulose template as a reference for the p-NOC before the reaction with calcium cations. *Insets* in the *upper right* indicate the fast Fourier transformed images. The cross section profiles along the perpendicular *A–B* are shown in the *bottom of* each figure. In (**a**, **b**), the average distances between two *parallel lines* were **a** ca. 0.17 μm and **b** ca. 0.14 μm. The *double arrows* indicate the stretching direction

in comparison between the two types of templates after reaction with calcium cations during immersion in a calcium buffer solution.

Elemental composition of mineral layers on cellulosic templates

Figure 2a and b profile X-ray photoelectron spectroscopy (XPS) survey spectra of the p-NOC templates before and after the reaction with calcium cations, together with commercially available hydroxyapatite (HAp) as a reference. In the XPS spectrum of the pre-reacted p-NOC template, both peaks of Ca due to calcium cations and P due to phosphate anions peaks were not detected (Fig. 2a). After the reaction with calcium cations by immersion for 10 min, Ca and P peaks (arrows in Fig. 2b) were clearly detected on the p-NOC template even after gentle washing with water. This profile of the spectrum corresponded well to that of HAp (Fig. 2c) (Michael et al. 1999), indicating formation of a calcium phosphate layer on the p-NOC surface.

Based on the above results, we will state a novel function of the p-NOC template as the phosphate anionic supply source in the following: Prior to the immersion in a calcium buffer solution, the initial

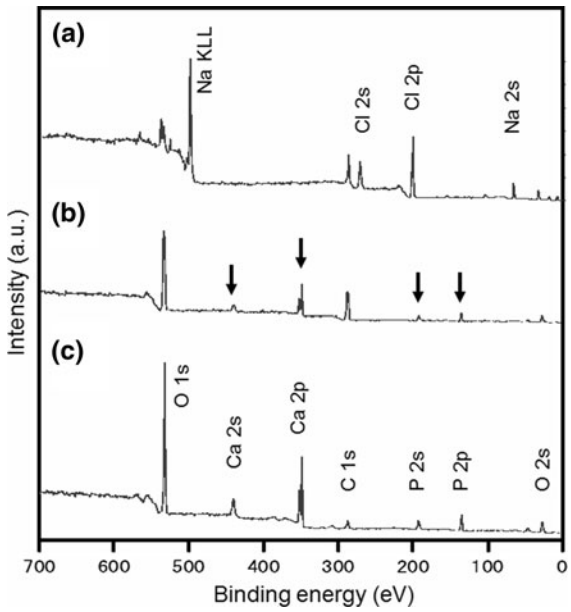

Fig. 2 XPS survey spectra of (*a*) p-NOC surface before the reaction with calcium cations, (*b*) p-NOC surface after reacted with calcium cations and (*c*) HAp as a reference

p-NOC templates were prepared to contain and immobilize the ions such as sodium cations, phosphate anions and chlorine anions, which were the components of the PBS solution. Once the p-NOC starts to be immersed in a calcium buffer solution, the ions might be transferred from inside to the surface of the p-NOC template, before calcium phosphates were generated by the preferential reaction of calcium cations with phosphate anions on the template. In other words, the p-NOC template played a part in supplying phosphate anions for formation of the calcium phosphates on the surface. Thus, the p-NOC template has been designed to exhibit a bio-mimic function as the phosphate anionic supply source.

Surface morphology and elemental composition of calcium-reacted p-NOC were concurrently investigated by using SEM-EDX system. Figure 3a shows the result of quantitative elemental analysis for the p-NOC surface after immersion to be reacted with calcium cations. The sodium, phosphorus, chlorine and calcium elements were detected by EDX. However, presence of the individual elements was not clearly identified on either surface or inside of the p-NOC template. Because the range of detection was limited in a few micro meters in depth, it was hard to measure the thin layer of the calcium phosphates having a few nano meters in depth. Figure 3b shows the SEM image of the p-NOC template after the reaction with calcium cations at 37 °C for 10 min. The groove, which was artificially split to expose the inside, was clearly appeared as shown in the center of the image. The rest smooth areas on the surface of the immersed p-NOC template were supposed to be the surface reacted with calcium cations. Since almost no mineral aggregate was observed on the inside areas (indicated as the groove) of the template, it was assumed that calcium-related deposits formed only on the surface of p-NOC substrates.

Elemental mappings on the p-NOC template (c-f) were performed for the same range as shown in Fig. 3b to identify where the individual elements were present. Elemental maps of calcium and phosphorus showed that the concentrations of calcium (Fig. 3c) and phosphorus (Fig. 3d) were significantly higher at the surface areas than the inside areas of p-NOC. On the other hand, both sodium (Fig. 3e) and chlorine (Fig. 3f) elements were spread over across the entire surface areas, indicating that there was not a significant difference in the same sodium and chlorine

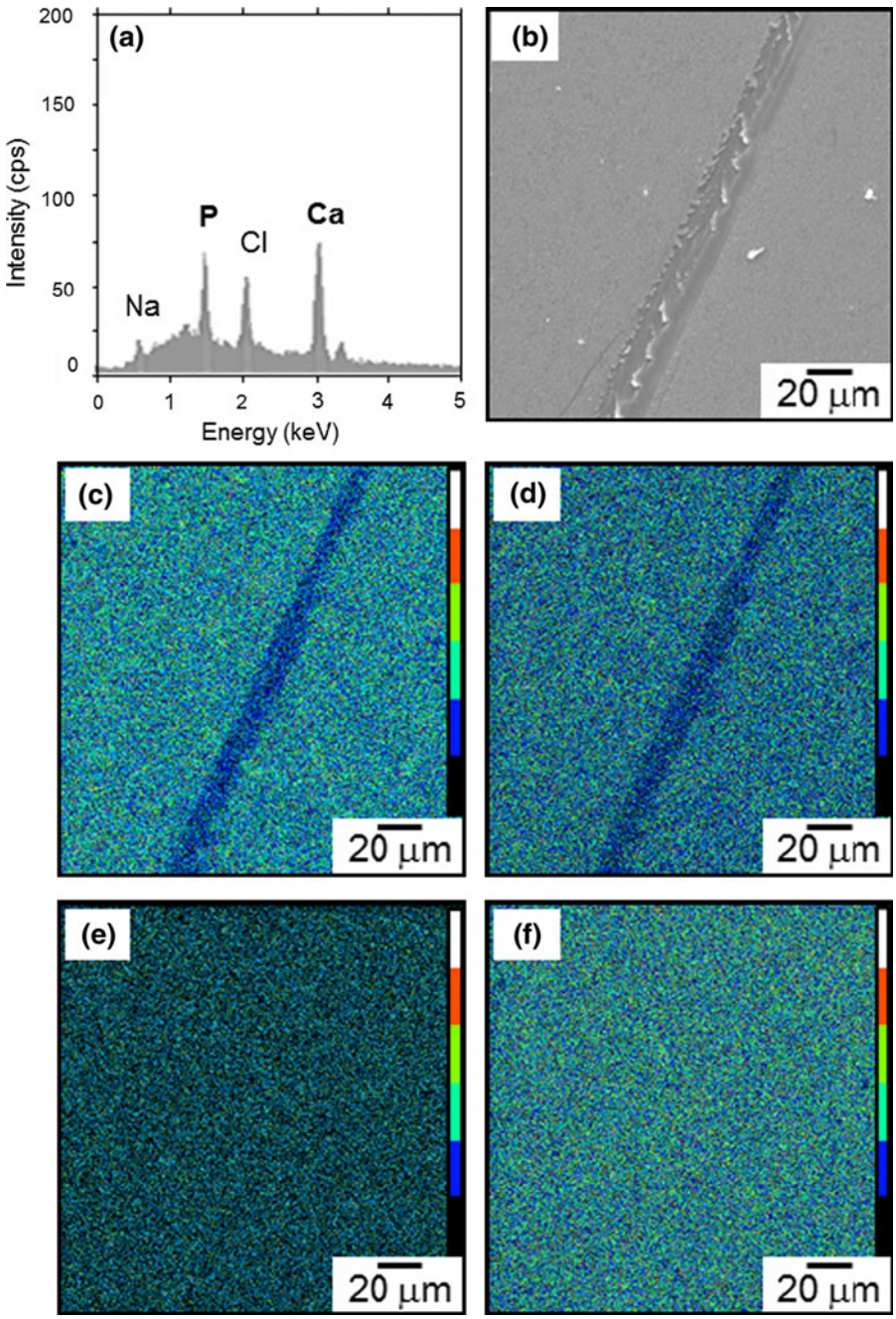

Fig. 3 EDX intensity profile **a** and the SEM image **b** of the p-NOC after reacted with calcium cations by immersion for 10 min together with the individual elemental mapping images of **c**–**f**: **a** EDX quantitative elemental analysis for the p-NOC template. **b** SEM image of the p-NOC surface with a crack where the inside of the film is exposed. Elemental mapping images of **c** calcium, **d** phosphorus, **e** sodium and **f** chlorine. In **c**–**f**, elemental concentrations are displayed as *inset bars* in the right. *White color* or *brighter colors* indicated a higher concentration

concentrations at both surface and inside of the p-NOC.

To quantify concentration of the individual element, the peak-to-background (p–b) ratio of the character X-rays intensity was obtained by point analysis for surface and inside of the p-NOC template. As listed in Table 1, elemental concentration of the calcium and phosphorus on the surface proved higher than that of the inside in p-NOC. In contrast, elemental concentration of the sodium and chlorine on the surface did not have a significant difference when compared with the inside in p-NOC. These results suggested that the calcium and phosphorus were major components present on the surface, whereas both of

Table 1 Peak-to-background (p–b) ratio of surface and inside of the p-NOC template calculated from the characteristic X-ray intensities

P–b ratio		
Element	Surface	Inside
Calcium	9.92 ± 1.66	6.24 ± 0.86
Phosphorus	4.15 ± 0.54	2.93 ± 0.31
Sodium	3.37 ± 0.47	3.40 ± 0.76
Chlorine	6.58 ± 0.75	6.25 ± 0.92

sodium and chlorine were distributed in the entire areas of the p-NOC.

Morphology of deposited calcium phosphate layers on cellulose templates

The surfaces of both p-NOC and non-ordered p-cellulose templates as a reference for the p-NOC after reacted with the calcium cations in the buffer solution were analyzed by using SEM observation. Figure 4a–c exhibit the surface morphological change of the p-NOC as elapse of the reaction time with calcium cations. Large amounts of the calcium phosphates were formed all over the surface of the p-NOC template after the reaction with calcium cations. In addition, the assembled pattern of the deposited minerals was well arranged along the molecular orientation of the p-NOC surface. The inset FFT images corresponding to each SEM image in Fig. 4a–c indicate that the longer the reaction time proceeded, the poorer the orientation of deposition of calcium phosphate aggregates became. The average distance between the oriented mineral lines (n = 50) was approximately 0.23 ± 0.07 μm (a), 0.19 ± 0.04 μm(b) and 0.30 ± 0.08 μm(c), respectively. These values were larger than that between the apparent tracks due to cellulose molecular chains on the p-NOC surface (see Fig. 1b: ca. 0.14 ± 0.03 μm (n=50)). The FFT image with a polar distribution confirms better orientation of the lines as shown in the inserted image in Fig. 4a–c, when compared with the inset of the non-ordered cellulose template as described below.

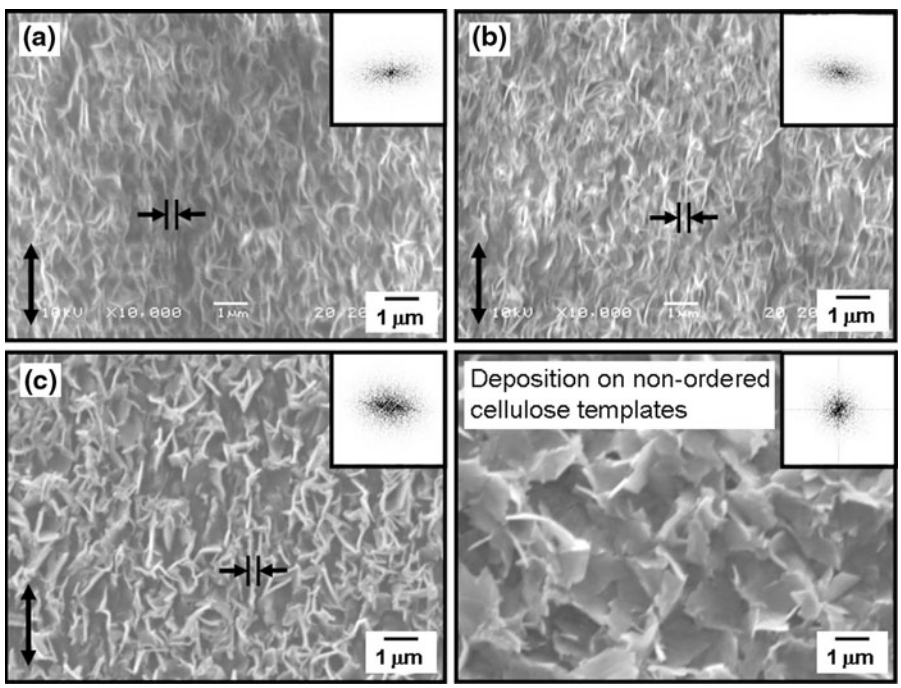

Fig. 4 SEM images of the surface of p-NOC templates after reactions with calcium cations for **a** 0.5, **b** 5.0 and **c** 10 min with the fast Fourier transformed images as insets in the right. The morphology of calcium phosphate deposition on the non-ordered cellulose template after the same reaction for 10 min is also displayed as a reference for the p-NOC template. In **a**–**c**, the *line* width of calcium phosphates was 0.23 ± 0.07 μm, 0.19 ± 0.04 μm and 0.30 ± 0.08 μm, respectively. The *double arrows* indicate the stretching direction

The calcium phosphates did not take any ordered shape on the surface of the non-ordered p-cellulose template as a reference for p-NOC, although large amounts of calcium phosphates were also formed all over the surface (see the SEM image in the right bottom of Fig. 4). In addition, the inserted FFT image of the non-ordered cellulose template exhibited randomly distributed spots, indicating that the deposition pattern of the calcium phosphates on the non-ordered template was not induced in a preferable manner. Accordingly, this result strongly suggests that the p-NOC surface encourages the uniaxially oriented deposition accompanied with synthesis of the calcium phosphates. It was obvious that the surface orientation of the p-NOC template mediated the orientation of the calcium phosphates, because of the correspondence with each other. However, the orientation of the inorganic deposits on the p-NOC surface tended to be reduced with the longer reaction time through a to c in Fig. 4.

Further, the particle size of calcium phosphates on the p-NOC template was smaller than those on the non-ordered p-cellulose template. It was presumably because a three-dimensional mineral deposition and its growth tended to be inhibited by the close contact of the uniaxially orientated cellulose molecular chains on p-NOC. The deposition of calcium phosphates was mostly limited to the orientation direction of the cellulose molecular chain, and thereby the shape of calcium phosphates was supposed to be also arranged along the stretching direction of p-NOC. It was a similar mechanism to a biomineralization with inhibition of the three-dimensional crystalline growth and the arrangement of the mineral shape mediated by orientated scaffolds such as collagen or chitin (Rho et al. 1998; Kato et al. 2002). In this way, the p-NOC template was considered as a bio-mimic template in terms of inducing orientation of calcium phosphates, as well as the phosphate anion supplier.

Crystallinity of deposited calcium phosphates on p-NOC templates

As described previously, the crystallinity of calcium phosphates was intergraded by the scaffold on a biomineralization. Therefore, examination for crystallinity of the deposited calcium phosphates was essential to estimate an impact of the scaffold on calcium phosphates. Figure 5 displays WAXD patterns of the calcium phosphate formed on the p-NOC template after reaction in a calcium buffer solution for 10 min, and the further sintered calcium phosphate. The calcium phosphates formed on the p-NOC template did not display any typical diffraction pattern of the crystalline phase. In contrast, the calcium phosphates after sintered showed the diffraction pattern ($2\theta = 31.0$ and 34.4°), similar to the typical diffraction pattern of the α-calcium phosphate tribasic (α-TCP) (2θ=23.1, 24.4, 31.0 and 34.4°) (Durucan and Brown 2000). This implied that the amorphous-to-crystalline transformation of the calcium phosphates occurred in the process of calcination at 800 °C. In other words, the deposited calcium phosphates were present as the amorphous phase on the p-NOC template after reacted with calcium cations in a buffer solution. This may be attributed to inhibition of the crystallization due to the close contact by a high adsorbability of the uniaxially orientated OH groups of cellulose molecular chains on the p-NOC surface, similarly to the case of the microbial crystalline cellulose nanofiber deposition on the NOC template as previously studied using *Gluconacetobacter xylinus* (Kondo et al. 2002; Kondo 2007). It should be noted that the dominant state of HAp in vivo on oriented collagen fibers as scaffolds in bones is also supposed to be amorphous (Roberts et al. 1991; Roberts et al. 1992).

When the p-NOC was immersed in a different calcium buffer solution (400 mM of $Ca(NO_3)_2{\cdot}4H_2O$/

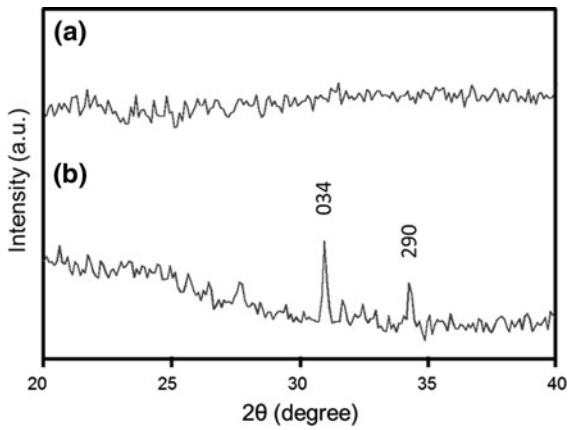

Fig. 5 WAXD patterns of (*a*) the synthesized calcium phosphates deposited on the p-NOC and (*b*) the sintered calcium phosphates of (*a*). In (*b*), the background intensity seen at $2\theta = 20$–28° is an experimental artifact from the tape for holding sample

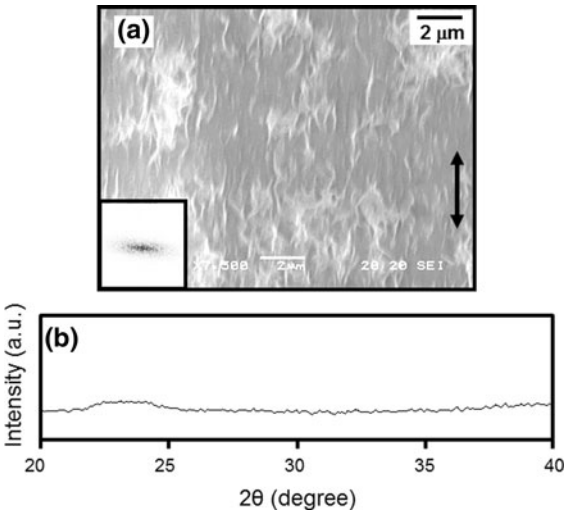

Fig. 6 SEM image **a** and WAXD intensity pattern **b** of the calcium nitrates deposited on the surface of p-NOC template after reaction with calcium cations in a different calcium buffer solution for 1.0 min. In **a**, the fast Fourier transformed image is inserted in the *left*. The *double arrow* indicates the stretching direction

Tris–HCl with pH 7.5), the surface orientation of the p-NOC template also mediated the uniaxially oriented deposition accompanied with synthesis of calcium nitrate instead of calcium phosphates, as shown in Fig. 6a. Further, the morphology of the oriented minerals in Fig. 6a was similar to that of Fig. 4a. This is because of the close reaction time between Fig. 6a and Fig. 4a. It seems that the p-NOC mediate the mineral deposition in the same way even if the inorganic composition is different. In fact, the orientation of calcium nitrates got worse with an increase of reaction time as seen in the case of calcium phosphates (data not shown). The WAXD patterns of the deposited calcium nitrates did not display any typical diffraction pattern of the crystalline phase (Fig. 6b). In this way, it is expected that the p-NOC could mediate the oriented deposition pattern of not only amorphous calcium phosphates but also various amorphous minerals.

Conclusion

This article attempted to propose an advanced possibility of NOC templates in terms of a novel biomineralization as a bifunctional cellulose template. In a previous paper, we emphasized that the surface of a unique form of cellulose, NOC, which was molecularly ordered, yet non-crystalline (Togawa and Kondo 1999; Kondo et al. 2001, 2002; Kondo 2007) could induce orientation of deposition of cellulose nanofibers secreted by *Gluconacetobacter xylinus*, a gram-negative bacterium (Kondo et al. 2002; Kondo 2007). Namely, the NOC played an important role as a scaffold for fabrication of the organic hierarchical structure as seen in living things.

In this study, we wished to extend the above concept of NOC further to fabrication of organic–inorganic hierarchical structure using a less energy consumption. Therefore, the NOC was at first modified into a bifunctional template containing phosphate anions for biomineralization, resulting in induction of oriented deposition of calcium phosphates as well as supplying the counter phosphate anions. Moreover, the uniaxially oriented calcium phosphates were found to be amorphous even though the deposition pattern was oriented along the surface orientation of the p-NOC. It should be noted that HAp in vivo that is mediated by the oriented collagen fibers is also supposed to be dominantly amorphous in human bones. Namely, the surface of p-NOC could mediate the mineralization process of calcium phosphates as a biomimic mineralization. Not only the case for calcium phosphate, it is expected that the biomimic mineralization using the modified NOC can also be applicable to the various kinds of minerals such as calcium nitrate and calcium carbonate by changing the reaction conditions in addition to the combination of the ions.

References

Anderson HC (1995) Molecular biology of matrix vesicles. Clin Orthop Relat Res 314:266–280

Boskey AL, Posner AS (1977) The role of synthetic and bone extracted calcium-phospholipid-phosphate complexes in hydroxyapatite formation. Calcif Tissue Res 23:251–258

Boyan BD, Schwartz Z, Swain LD, Khare A (1989) Role of lipids in calcification of cartilage. Anat Rec 224:211–219

Dorozhkin SV, Epple M (2002) Biological and medical significance of calcium phosphates. Angewandte Chemie Int Edn 41:3130–3146

Durucan C, Brown PW (2000) α-tricalcium phosphate hydrolysis to hydroxyapatite at and near physiological temperature. J Mater Sci Mater Med 11:365–371

Furuzono T, Taguchi T, Kishida A, Tamada Y (2000) Preparation and characterization of apatite deposited on silk fabric using an alternate soaking process. J Biomed Mater Res 50:344–352

Jie S, Viengkham M, Carolyn RB (2005) Mineralization of synthetic polymer scaffolds: a bottom-up approach for the development of artificial bone. J Am Chem Soc 127:3366–3372

Kato T, Sugawara A, Hosoda N (2002) Calcium carbonate-organic hybrid materials. Adv Mate. 14:869–877

Kim HM, Rey C, Glimcher MJ (1996) X-ray diffraction, electron microscopy, and Fourier transform infrared spectroscopy of apatite crystals isolated from chicken and bovine calcified cartilage. Calcif Tissue Int 59:58–63

Kokubo T (1990) Surface chemistry of bioactive glass-ceramics. J Non-Cryst Solids 120:138–151

Kokubo T (2005) Design of bioactive bone substitutes based on biomineralization process. Mat Sci Eng C 25:97–104

Kondo T (2007) Nematic ordered cellulose: its structure and properties. In: Brown RM Jr, Saxena IM (eds) Cellulose: molecular and structural biology. Springer, New York, pp 285–305

Kondo T, Togawa E, Brown RM Jr (2001) "Nematic ordered cellulose": a concept of glucan chain association. Biomacromolecules 2:1324–1330

Kondo T, Nojiri M, Hishikawa Y, Togawa E, Romanovicz D, Brown RM Jr (2002) Biodirected epitaxial nano deposition of polymers on oriented macromolecular templates. Proc Natl Acad Sci USA 99:14008–14013

LeGeros RZ (2002) Properties of osteoconductive biomaterials: calcium phosphates. Clin Orthop Relat Res 395:81–98

Michael J, Van S, Dina RJ, Emile AS (1999) Calcium phosphate phase identification using XPS and time-of-flight cluster SIMS. Anal Chem 71:149–153

Olszta MJ, Cheng XG, Jee S-S, Kumar R, Kim Y-Y, Kaufman MJ, Douglas EP, Gower LB (2007) Bone structure and formation: a new perspective. Mat Sci Eng R Rep 58: 77–116

Rho JY, Kuhn-Spearing L, Zioupos P (1998) Mechanical properties and the hierarchical structure of bone. Med Eng Phys 20:92–102

Roberts JE, Heughebaert M, Heughebaert JC, Bonar LC, Glimcher MJ, Griffin RG (1991) Solid State ^{31}P NMR Studies of the conversion of amorphous tricalcium phosphate to apatitic tricalcium phosphate. Calcif Tissue Int 49:378–382

Roberts JE, Bonar LC, Griffin RG, Glimcher MJ (1992) Characterization of very young mineral phases of bone by solid state ^{31}Phosphorus magic angle sample spinning nuclear magnetic resonance and X-ray diffraction. Calcif Tissue Int 50:42–48

Taguchi T, Kishida A, Akashi M (1998) Hydroxyapatite formation on/in poly (vinyl alcohol) hydrogel matrices using a novel alternate soaking process. Chem Lett 8:711–712

Togawa E, Kondo T (1999) Change of morphological properties in drawing water-swollen cellulose films prepared from organic solutions. A view of molecular orientation in the drawing process. J Polym Sci B Polym Phys 37:451–459

Weiner S, Wagner HD (1998) The material bone: structure-mechanical function relations. Annu Rev Mat Sci 28: 271–298

Yokota S, Kitaoka T, Wariishi H (2007) Surface morphology of cellulose films prepared by spin coating on silicon oxide substrates pretreated with cationic polyelectrolyte. Appl Surf Sci 253:4208–4214